



# Kinetics of oxidation roasting of molybdenite with different particle sizes

Xiao-bin LI, Tao WU, Qiu-sheng ZHOU, Tian-gui QI, Zhi-hong PENG, Gui-hua LIU

School of Metallurgy and Environment, Central South University, Changsha 410083, China

Received 5 May 2020; accepted 18 October 2020

**Abstract:** The kinetics of oxidation roasting of molybdenum concentrate was studied by differential thermal-gravimetric experiments and non-isothermal analysis methods. The results show that high temperature is beneficial for oxidation of molybdenum concentrate. The initial oxidation temperature of the molybdenum concentrate is 450 °C, and the rapid oxidation occurs above 500 °C. The oxidation process conforms to the unreacted shrinking nucleus model. The early stage of the oxidation is controlled by chemical reaction with the apparent activation energy of 123.180 kJ/mol, while the later stage is controlled by internal diffusion with the apparent activation energy of 80.175 kJ/mol. Moreover, the oxidation rate is closely related to particle size of the concentrate. The smaller the particle size is, the larger the oxidation rate is.

**Key words:** molybdenite; oxidation; roasting; kinetics; particle size

## 1 Introduction

Molybdenum is widely used in materials and chemical industry [1,2]. Molybdenite is the main mineral of molybdenum, and its extraction is divided into pyro process and hydro process according to oxidation methods. The later mainly includes nitric acid leaching [3,4], pressure acidic/alkaline leaching [5,6], sodium hypochlorite/dichromate leaching [7,8], and electrochemical leaching [9]. The hydro process has advantages of strong adaptability to raw materials and low environmental pollution. However, it is not mature in industrial applications because of harsh equipment requirement and high operation costs. As for the pyrolytic process, it can be categorized according to the types of additives, such as direct oxidation roasting, lime roasting [10], sodium/magnesium carbonate roasting [11–13], chlorination roasting [14–16], and hydrogen reduction [17–20]. Direct oxidation roasting using air as an oxidant is the prevalent method due

to less investment and low operation costs, whereas the oxidation product  $\text{MoO}_3$  readily sublimates above 600 °C causing loss of molybdenum. Moreover, low melting point eutectic with impurity metal oxides and sinter readily form, seriously deteriorating the roasting process. When roasted at relatively lower temperatures, the oxidation is slow, resulting in low conversion rate [21]. To address this problem, many scholars studied kinetics of oxidation roasting of molybdenum concentrates. GAN et al [22] reported the effects of calcium-based additives on the roasting of low-grade molybdenum concentrates. They found that the initial oxidation temperature of  $\text{MoS}_2$  is 450 °C while the formations of  $\text{CaMoO}_4$  and  $\text{CaSO}_4$  occur above 500 °C. Increasing temperature accelerates  $\text{CaMoO}_4$  formation but decreases both sulfur fixation rate and molybdenum retention rate. WILKOMIRSKY et al [23] studied calcination kinetics of molybdenite with particle size of 35–53  $\mu\text{m}$  at different oxygen concentrations and temperatures. Their results show that the calcination is a first-order reaction, follows the unreacted

shrinking core model, and is controlled by chemical reactions with activation energy of 104.0 kJ/mol. Additionally, YANG et al [24] examined the oxidation kinetics by the thermogravimetric–differential thermal experiments, and concluded that the oxidation is controlled by internal diffusion at low temperatures and by chemical reaction at high temperatures. But the boundary between the two steps was not studied in depth, and the effect of particle size on the shrinking core model was not considered.

In summary, the researches on kinetics of oxidaton roasting of molybdenum concentrates were mainly focused on the kinetic parameters and roasting mechanism. It is generally believed that the molybdenite oxidation conforms to the shrinking core model and is controlled by either internal diffusion or chemical reaction. However, few studies were conducted on the control steps and particle size effect. Practically, the particle size often has a great impact on the oxidation. Therefore, the kinetics of oxidation roasting of molybdenite with different particle sizes was studied in this work through differential heat-thermogravimetry experiments. The research clarified the control steps, boundary and particle size effect. The findings presented may provide further theoretical base for industrial direct oxidation of molybdenum concentrate.

## 2 Experimental

### 2.1 Materials

The molybdenum concentrate was provided by Chengdu Hongbo Molybdenum Co., Ltd., China. The main chemical compositions and X-ray diffraction pattern of the concentrate are shown in Table 1 and Fig. 1, respectively.

From Table 1, it can be seen that the concentrate has molybdenum content of 45.85% and S content of 31.01%. Other impurities mainly include Ca, Cu, Si, Pb, and P. XRD analysis shows that Mo and S exist mainly in the form of MoS<sub>2</sub> in the concentrate, and the impurity element Si mainly

**Table 1** Main chemical compositions of molybdenum concentrate (wt.%)

Mo	S	H <sub>2</sub> O	Ca	Cu	Si	Pb	P
45.85	31.01	10.72	1.40	1.20	2.10	0.77	0.04

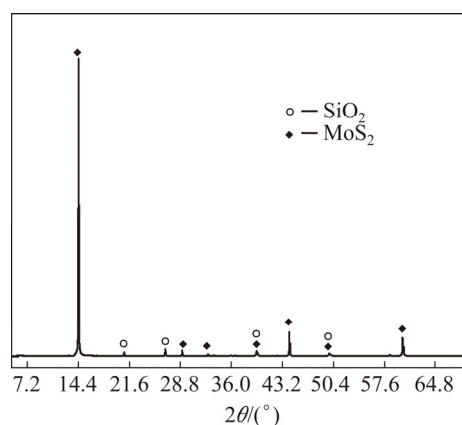


**Fig. 1** XRD pattern of molybdenum concentrate

in the form of quartz. Other metal impurities are not detected in XRD analysis and may be in the form of oxides or sulfides.

### 2.2 Experimental methods

The dried molybdenum concentrate was divided into different particle sizes of <75, 75–106, 106–150 and 150–250 μm. The SDTQ600 thermal analyzer was used to perform differential thermal-gravimetric analyses in air. The heating rate is 10 °C/min, and the temperature range is 25–800 °C. The thermogravimetric curve (TG) and heat flow curve (DSC) were obtained to compare the reaction behavior of the molybdenum concentrate with different particle sizes during roasting.

### 2.3 Selection of non-isothermal thermodynamic analysis methods

The oxidation process of molybdenite concentrate in thermal analysis experiments is a non-isothermal reaction process, and the reaction temperature is a function of time. For kinetic data processing methods of non-isothermal processes, the Kissinger method, FWO method and Coats–Redfern integral method are frequently used.

(1) Kissinger and FWO methods [25–27]

The derivation formulas of Kissinger method and FWO method are listed respectively as follows:

$$\ln\left(\frac{\beta}{T_p^2}\right) = \ln\left(\frac{AR}{E_a}\right) - \frac{E_a}{RT_p} \quad (1)$$

$$\ln\beta = \lg\left(\frac{AE_a}{Rg(a)}\right) - 2.315 - 0.456\frac{E_a}{RT} \quad (2)$$

where  $\beta$  is the heating rate,  $T_p$  is the peak temperature of the differential TG curve (DTG),  $A$

is the pre-exponential factor,  $R$  is the gas constant,  $T$  is the thermodynamic temperature,  $g(a)$  is the integral form of reaction model with the maximum correlation coefficient, and  $E_a$  is the activation energy. By fitting the linear relationship between  $\ln(\beta/T_p^2)$  (or  $\lg \beta$ ) and  $1/T$  via the least square method,  $E_a$  and  $A$  can be calculated by the slope and intercept of the line. The advantage of both the Kissinger method and the FWO method is that the influence of the reaction model is not taken into account in the calculation, but such a simplified processing may result in a larger error of the calculated value.

### (2) Coats–Redfern integral method [28]

The Coats–Redfern integral method is the most commonly used method for studying the non-isothermal reaction mechanism functions, and the formula is

$$\ln \frac{F(x)}{T^2} = \ln \left[ \frac{AR}{\beta E} \left( 1 - \frac{2RT}{E} \right) \right] - \frac{E}{RT} \quad (3)$$

where  $F(x)$  is reaction mechanism function.

$x$  is the oxidation ratio at different temperatures in the non-isothermal process, and can be calculated by the mass changes in TG curves.

$$x = \frac{w_0 - w_T}{w_0 - w_\infty} \quad (4)$$

where  $w_0$ ,  $w_T$  and  $w_\infty$  represent the initial mass, the mass at temperature  $T$ , and the mass after reaction completion of the concentrate, respectively.

For most conditions,  $E$  is much greater

than  $2RT$ , namely  $\ln \left[ \frac{AR}{\beta E} \left( 1 - \frac{2RT}{E} \right) \right]$  can be

considered as a constant. For a particular  $F(x)$ , a linear relationship between  $\ln[F(x)/T^2]$  and  $1/T$  can be obtained by the linear fitting, and  $E$  and  $A$  can thus be calculated respectively according to the slope and intercept of the fitted line. As the influence of reaction mechanism on calculation results is fully considered when applying the Coats–Redfern integral method, the subsequent kinetic parameters are calculated by this method.

## 3 Results and discussion

### 3.1 TG–DSC analysis of molybdenite concentrate

Figure 2 shows the TG–DSC curves of oxidation of molybdenite concentrate with different

particle sizes. TG curve shows that mass loss of concentrate occurs in two different temperature ranges with the temperature rising. At the low temperatures (350–550 °C), the concentrate mass changes little (<450 °C) and then decreases remarkably. Moreover, the mass change rate of small-size concentrate is much greater than that of the large-size one (>450 °C). At the high temperatures (550–800 °C), the mass change of the large-size concentrate increases sharply with the mass loss greater than 35% at 800 °C for 150–250 μm. The DSC curve shows that there is an obvious exothermic peak at 500 °C, indicating that the chemical reaction occurs at 500 °C.

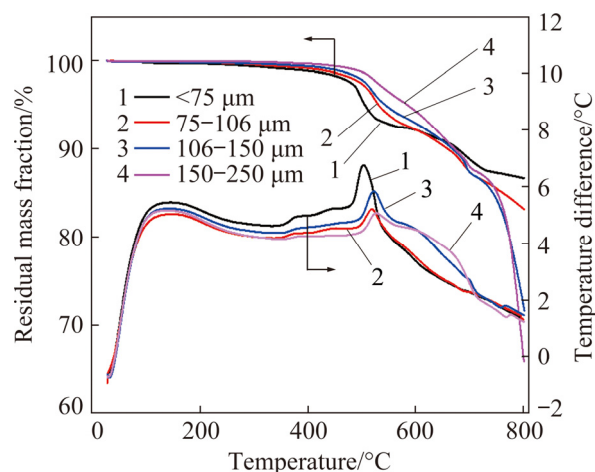


Fig. 2 TG–DSC curves of molybdenite concentrate

The physicochemical reaction in the roasting process is further analyzed, in which the chemical reaction is the REDOX reaction of  $\text{MoS}_2$  as well as the reactions of molybdenum trioxide with impurity metal oxides to form molybdates:



Thermodynamic calculation shows that these reactions can occur within 1000 °C. When  $\text{MoS}_2$  is completely reacted, the theoretical mass reduction of molybdenite is 8.5%, which is well consistent with the mass change in the low temperature range. Additionally, the exothermic peak appears in this temperature range, further verifying that the oxidation of molybdenite occurs mainly in this range. The sublimation temperature of molybdenite trioxide is 600 °C, so the significant mass change in the high temperature range is mainly attributed to the sublimation of molybdenum trioxide.

In order to eliminate the influence of the sublimation on experimental results, 350–550 °C was chosen as the calculated temperature range. The oxidation ratio ( $x$ ) and oxidation rate ( $dx/dt$ ) of molybdenite in the temperature range were calculated according to the mass changes of TG curves in Fig. 2.

As shown in Fig. 3, the initial oxidation temperature of molybdenite is approximately 450 °C. For a specific particle size, the oxidation ratio is accelerated first and then slowed down. Furthermore, the smaller the particle of the concentrate, the higher the oxidation ratio. For the same temperature, the oxidation ratio of small particle molybdenite is larger than that of the larger

one. The oxidation ratio for particle size less than 75  $\mu\text{m}$  reaches 92.80% at 550 °C. Similarly, the oxidation rate in Fig. 4 shows the same trend as the oxidation ratio. There is an obvious inflection point for the oxidation rate, and this inflection point is often accompanied by changes in the kinetic control steps, which need to be verified by the following calculations.

### 3.2 Non-isothermal kinetic analysis

Figure 5 shows the EDS results of roasted products of the concentrate with different particle sizes. The results illustrate that the roasted products can be divided into three types: white products, mixed products and gray products. The

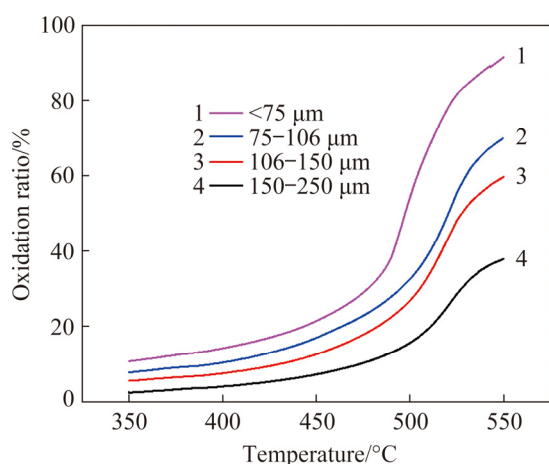


Fig. 3 Curves of oxidation ratio of molybdenite

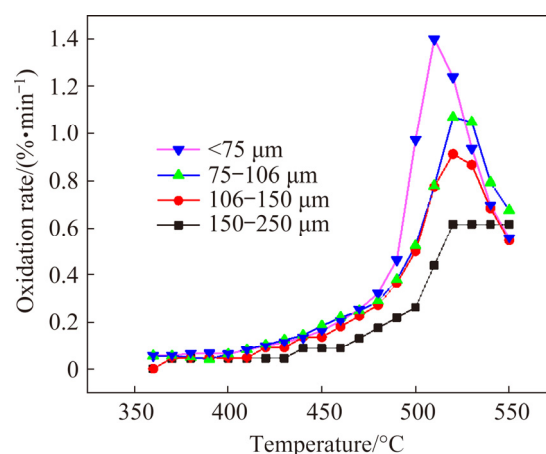


Fig. 4 Curves of oxidation rate of molybdenite

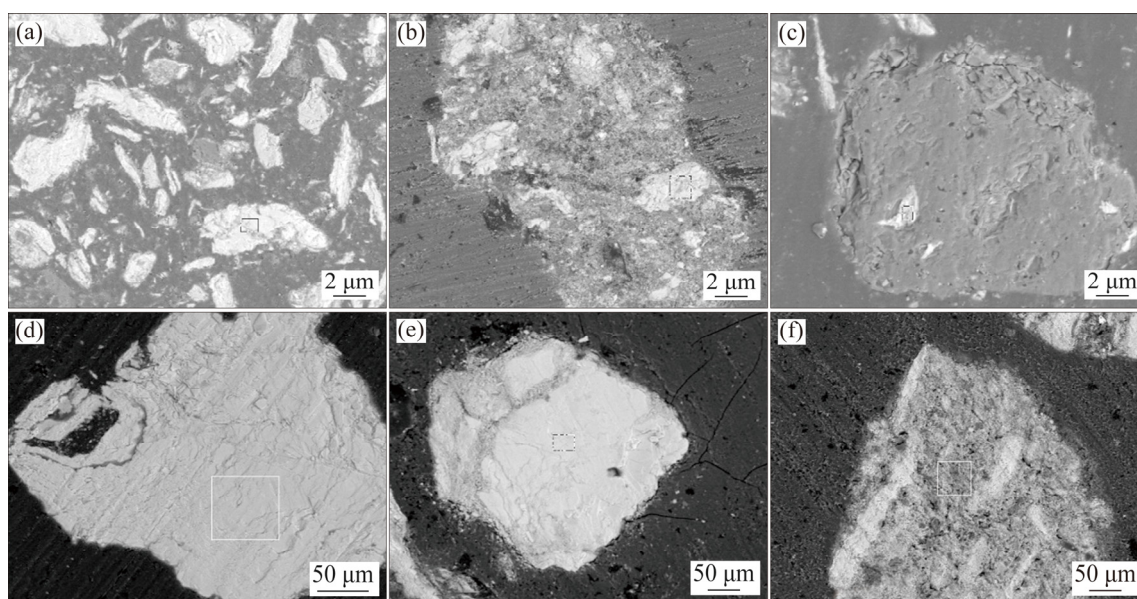


Fig. 5 EDS results of roasted products of molybdenite concentrate with different particle sizes roasted in muffle furnace for different time: (a) <75  $\mu\text{m}$ , 0 min; (b) <75  $\mu\text{m}$ , 5 min; (c) <75  $\mu\text{m}$ , 20 min; (d) 150–250  $\mu\text{m}$ , 0 min; (e) 150–250  $\mu\text{m}$ , 5 min; (f) 150–250  $\mu\text{m}$ , 20 min

compositions analyzed by the electron probe suggest that the white area is unreacted molybdenum sulfide, the mixed area is a mixture of sulfur, molybdenum and oxygen, and the gray area is molybdenum trioxide.

Figures 5(a, d) manifest that the original molybdenite concentrate is composed of white molybdenum sulfide. From Figs. 5(b, e, f), the concentrate roasted for a certain time consists of white area and mixture area. Moreover, the mixture seems to form a product layer on the periphery and wraps the unreacted white molybdenum sulfide. Since these mixtures are not dense, oxygen is easy to enter the particles during roasting and reacts with molybdenum sulfide, and the reaction ratio can be further increased. In Fig. 5(c), as the fine concentrate is roasted for a relatively long time, the mixture is completely oxidized to molybdenum trioxide and a dense oxide film is formed on the surface of molybdenite sulfide. This makes the diffusions of oxygen and  $\text{SO}_2$  difficult and thus the enclosed molybdenum sulfide is difficult to be oxidized, which will definitely inhibit the oxidation of molybdenite.

The gas–solid reaction that produces dense products can be treated with an unreacted shrink nucleus model. The main control steps of the reaction are external diffusion, internal diffusion and chemical reaction. The reaction kinetics equations of different control steps are given in Table 2.

**Table 2** Kinetic equations of reaction

Name	Kinetic equation	Control step
$F_1(x)$	$1-(1-x)^{1/3}=k_1t$	Chemical reaction
$F_2(x)$	$1-(1-x)^{2/3}=k_2t$	External diffusion
$F_3(x)$	$1-2x/3-(1-x)^{2/3}=k_3t$	Internal diffusion

$x$  is the reaction ratio,  $t$  is the reaction time, and  $k$  is the reaction rate constant

According to the integral formula of Coats–Redfern, for its kinetic equation  $F(x)$ , the better the linear relationship between calculated  $\ln[F(x)/T^2]$  and  $1/T$ , the closer the kinetic model is to the actual situation. The reaction ratio  $x$  of oxidation roasting of molybdenite concentrate with different particle sizes in Fig. 3 is substituted into the mechanism function  $F(x)$  under different control steps in Table 2, and the linear fitting of  $\ln[F(x)/T^2]$  to  $1/T$  is performed within the temperature range of

450–550 °C. The fitting results for particle size of <75  $\mu\text{m}$  are plotted in Fig. 6.

Figure 6 shows that when linear fitting is performed with different kinetic equations, the inflection points on the fitting curves appear at around 500 and 525 °C, revealing that the kinetic control steps during REDOX of the concentrate in different temperature ranges are not the same.

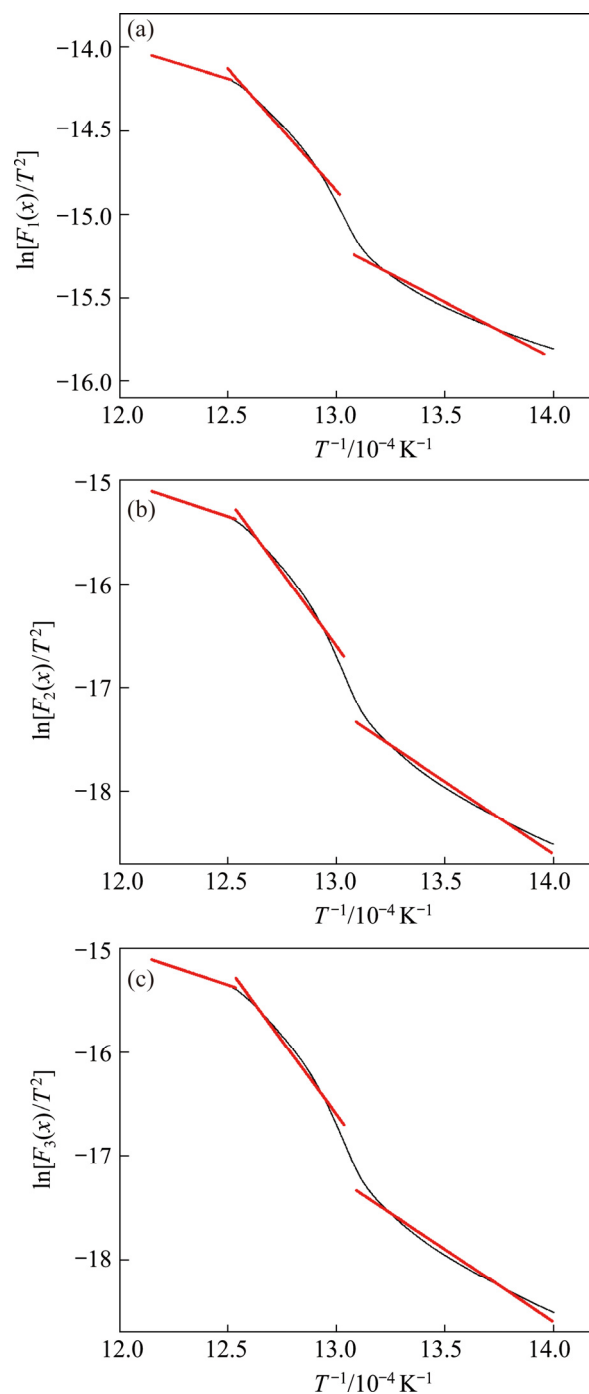


**Fig. 6** Linear fitting results of  $\ln[F(x)/T^2]$  to  $1/T$  under different control steps for concentrate particle size of <75  $\mu\text{m}$ : (a) Chemical reaction control; (b) External diffusion control; (c) Internal diffusion control

Therefore, the kinetic equations in different temperature ranges are fitted linearly according to the inflection point. Considering the influence of unstable interval on the results during the transition of different control steps, the change within 450–490 °C is taken as the first step, the change within 500–525 °C as the second step, and the change within 530–550 °C as the third step. The fitting results of the maximum linear correlation coefficient are taken as the experimental result, and listed in Table 3.

Table 3 shows the activation energy  $E_a$  of molybdenite oxidation roasting for each particle size with different kinetic equations, where  $R^*$  denotes linear correlation coefficient. It is found that the correlation is good after linear treatment with external diffusion, chemical reaction or internal diffusion equation in different temperature ranges. Considering that the experiment was done in a thermal analyzer where the gas diffused quickly, the external diffusion is not a control step. At 450–490 °C, the oxidation ratio is low and the oxidation rate is accelerated, but the DSC curve shows no obvious exothermic peak in this temperature range. This implies that the oxidation reaction is in an induction phase and controlled by chemical reaction in this range. At 500–525 °C, the oxidation rate of molybdenite gets faster and there is an obvious exothermic peak on the DSC curve, suggesting that molybdenite is rapidly oxidized

under chemical reaction control in this range. After a certain duration of chemical reaction, the surface product layer formed on molybdenite particles retards oxygen internal diffusion and the reaction rate drops sharply, where the reaction is diverted to internal diffusion control at 530–550 °C.

### 3.3 kinetics of oxidizing roasting of molybdenite concentrate

#### 3.3.1 Calculation of thickness of product layer

The oxidation reaction is composed of several steps. When estimating the reaction behavior, it is necessary to know the critical conditions for the conversion of each control step, especially for the conversion from chemical reaction control to internal diffusion control. If molybdenite particles have the same size in all directions with the same chemical activity, they can be considered as spheres with a radius of  $r_0$ . As the oxidation goes on, the unreacted particle has a radius of  $r$  at time  $t$ . The chemical reaction rate  $v$  can be expressed by

$$v = -\frac{dm}{dt} = kSC^n \quad (7)$$

where  $m$  is the mass of the unreacted nucleus at time  $t$ ,  $k$  is the rate constant of surface chemical reaction,  $S$  is the reaction interface area ( $m^2$ ),  $C$  is the reactant concentration (mol/L), and  $n$  is the reaction order. For molybdenite concentrate,  $C^n$  could be considered as a constant.

**Table 3** Kinetic parameters of oxidation process of molybdenite concentrate

Particle size/ $\mu\text{m}$	Mechanism function	First step			Second step			Third step		
		$E_a/(\text{kJ}\cdot\text{mol}^{-1})$	$A$	$(R^*)^2$	$E_a/(\text{kJ}\cdot\text{mol}^{-1})$	$A$	$(R^*)^2$	$E_a/(\text{kJ}\cdot\text{mol}^{-1})$	$A$	$(R^*)^2$
<75	$F_1(x)$	56.15	111.1	0.9687	121.5	$9.195\times 10^6$	0.9824	41.51	17.73	0.9966
	$F_2(x)$	51.66	134.4	0.9560	113.57	$3.988\times 10^4$	0.9468	24.46	1.252	0.9529
	$F_3(x)$	116.4	$3.574\times 10^5$	0.9775	235.1	$1.618\times 10^{14}$	0.9796	78.32	2626	0.9984
75–106	$F_1(x)$	49.35	24.80	0.9946	124.1	$7.156\times 10^6$	0.9935	47.21	27.82	0.9516
	$F_2(x)$	46.99	30.95	0.9953	105.8	$6.868\times 10^5$	0.9921	41.07	16.55	0.9511
	$F_3(x)$	106.6	$4.197\times 10^4$	0.9964	238.0	$7.713\times 10^{13}$	0.9933	80.54	1592	0.9865
106–150	$F_1(x)$	57.47	81.03	0.9952	124.1	$5.988\times 10^6$	0.9943	43.77	25.79	0.9716
	$F_2(x)$	56.55	133.8	0.9940	117.4	$3.763\times 10^6$	0.9977	32.40	3.005	0.9765
	$F_3(x)$	126.2	$6.846\times 10^5$	0.9952	256.5	$9.889\times 10^{14}$	0.9984	80.38	1034	0.9873
150–250	$F_1(x)$	55.27	30.49	0.9948	123.0	$2.747\times 10^6$	0.9964	47.63	13.37	0.9479
	$F_2(x)$	54.36	51.01	0.9945	118.0	$2.329\times 10^6$	0.9967	48.93	30.07	0.9511
	$F_3(x)$	126.5	$2.303\times 10^5$	0.9936	255.7	$2.670\times 10^{14}$	0.9977	81.46	422.8	0.9707

$R^*$ —Linear correlation coefficient

Then, the differential equation can be readily obtained as follows:

$$-\frac{dm}{dt} = -4\pi r^2 \rho \frac{dr}{dt} \quad (8)$$

where  $\rho$  is the density of molybdenite concentrate. So,

$$r_0 - r = k \frac{C_0^n}{\rho} t \quad (9)$$

where  $k$ ,  $C_0$  and  $\rho$  are all constants at the same temperature. Therefore, while molybdenum is oxidized under chemical reaction control, the thickness of product layer is the same at the same time. When the oxidation is changed into internal diffusion control from chemical control, the product layer is formed outside the nucleus. The thickness of the product layer is assumed to be  $\delta$  and it can be calculated by the rate inflection point. For the concentrate with particle size of  $<75 \mu\text{m}$ , its particle size distribution is shown in Fig. 9, and its particle size distribution function is  $f(r)$ . The temperature at its inflection point is  $525 \text{ }^\circ\text{C}$  corresponding to the oxidation ratio of  $81.55\%$ , and the mass of molybdenite of  $<75 \mu\text{m}$  with a certain number of particles  $m_0$  is

$$m_0 = \sum_{r_1}^{r_2} \frac{4}{3} \rho \pi r^3 f(r) \quad (10)$$

The mass of the unreacted nucleus is

$$m = \sum_{\delta}^{r_2} \frac{4}{3} \rho \pi (r - \delta)^3 f(r) \quad (11)$$

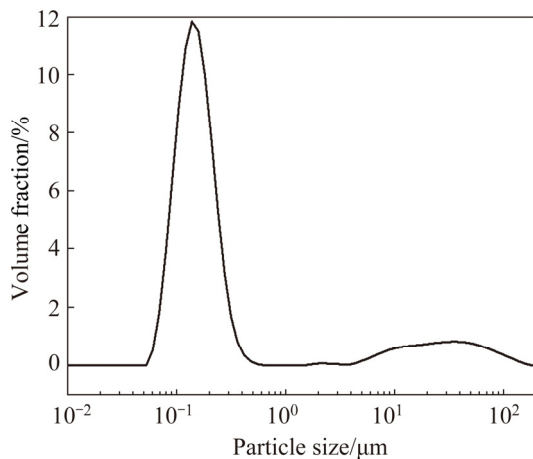


Fig. 9 Particle size distribution curve of molybdenite concentrate ( $<75 \mu\text{m}$ )

Considering the unreacted rate,  $m/m_0$ , is  $0.1845$ , the thickness  $\delta$  is thus calculated to be approximately  $40 \mu\text{m}$ . Similarly, the thickness of molybdenite with different particle sizes can also be calculated. It is found that the product layer thickness for molybdenite with different particle sizes is  $40\text{--}56 \mu\text{m}$ , disclosing that the surface energy and chemical properties of molybdenum concentrate with different particle size are almost the same and the same rules should be followed in the oxidation.

Based on the above theoretical calculation, during the oxidizing roasting of molybdenite concentrate with different particle sizes, the oxidation is controlled only by chemical reaction for particle size less than  $\delta$ , and by chemical reaction and subsequent internal diffusion for particle size greater than  $\delta$ .

### 3.3.2 Determination of kinetic equation of chemical reaction control

As can be seen from Table 3, when the oxidation is controlled by chemical reaction, the apparent activation energy of molybdenite concentrate with different particle sizes is basically the same, and their average value of  $123.18 \text{ kJ/mol}$  is taken as the activation energy of the chemical reaction. The kinetic equation of the chemical reaction for different particle sizes can be expressed as follows:

$$K_{<75 \mu\text{m}} = 9.20 \times 10^6 \exp[-123180/(8.314T)]$$

$$K_{75\text{--}106 \mu\text{m}} = 7.18 \times 10^6 \exp[-123180/(8.314T)]$$

$$K_{106\text{--}150 \mu\text{m}} = 5.99 \times 10^6 \exp[-123180/(8.314T)]$$

$$K_{150\text{--}250 \mu\text{m}} = 4.22 \times 10^6 \exp[-123180/(8.314T)]$$

According to the kinetic equation of chemical reaction control,

$$1 - (1-x)^{1/3} = k_1 t \quad (12)$$

In combination with Eq. (9), for a single particle with the volume of  $V$ ,  $k_1$  can be expressed as

$$k_1 = \frac{kC^n}{\rho r_0} = \frac{kS}{V\rho} \quad (13)$$

For molybdenum concentrate with dispersed particle size,  $r_0$  is difficult to determine, so the specific surface area of  $S_0/V_0$  can be used to represent the relationship between  $k_1$  and particle size distribution, as shown in Eq. (14):

$$k_1 \propto \frac{S_0}{V_0} \quad (14)$$

where  $S_0$  (total surface area) and  $V_0$  (total volume) for molybdenite concentrate with different particle size distribution can be calculated by Eqs. (15) and (16), respectively. The diagram of  $k_1$  versus  $S_0/V_0$  is shown in Fig. 10.

$$S_0 = \sum_{r_1}^{r_2} 4\pi r^2 f(r) \quad (15)$$

$$V_0 = \sum_{r_1}^{r_2} \frac{4}{3} \pi r^3 f(r) \quad (16)$$

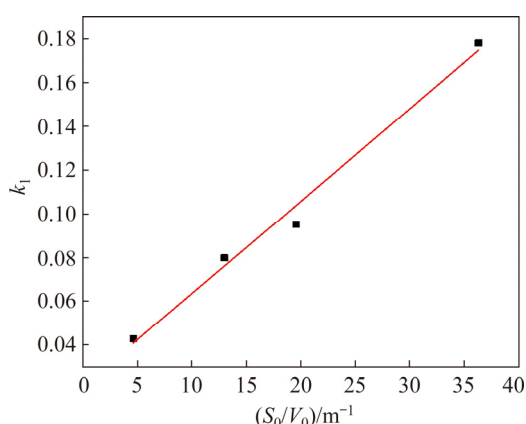


**Fig. 10** Diagram of  $k_1$  vs  $S_0/V_0$  under chemical reaction control at 525 °C

In Fig. 10, the correlation coefficient of the fitting line is 0.984, and the relation between  $k_1$  and  $S_0/V_0$  is

$$k_1 = 2.17 \times 10^5 (S_0/V_0 + 5.02) \exp[-123180/(8.314T)] \quad (17)$$

Therefore, the kinetic equation of chemical reaction control is

$$1 - (1-x)^{1/3} = 2.17 \times 10^5 (S_0/V_0 + 5.02) \times \exp[-123180/(8.314T)] t \quad (18)$$

### 3.3.3 Determination of kinetic equation of internal diffusion control

Table 3 shows that the apparent activation energy of internal diffusion for different sizes is basically the same. Similarly, the average value of 80.175 kJ/mol is taken as the activation energy of the internal diffusion, where  $K$  can be expressed as follows:

$$K_{<75 \mu m} = 2626 \exp[-80175/(8.314T)]$$

$$K_{75-106 \mu m} = 1592 \exp[-80175/(8.314T)]$$

$$K_{106-150 \mu m} = 1034 \exp[-80175/(8.314T)]$$

$$K_{150-250 \mu m} = 422.8 \exp[-80175/(8.314T)]$$

According to the kinetic equation (Eq. (19)) of internal diffusion control,

$$1 - 2x/3 - (1-x)^{2/3} = k_2 t \quad (19)$$

The internal diffusion rate constant  $k_2$  can be expressed as Eq. (20) for individual particles:

$$k_2 = \frac{2DC_0}{r_0^2 a \rho} = \frac{2DC_0 S_0^2}{V_0^2 a \rho} \quad (20)$$

where  $a$  is a proportional coefficient.

Likewise, the item  $(S_0/V_0)^2$  can be used to represent the relationship between  $k_2$  and particle size distribution:

$$k_2 = k' (S_0/V_0)^{2n'} \exp[-E/(RT)] \quad (21)$$

where  $k'$  is the frequency factor,  $n'$  is the shape factor of molybdenum concentrate particles. After calculation of  $S_0$  and  $V_0$ , the diagram of  $\ln k_2$  versus  $\ln(S_0/V_0)$  is then plotted, as shown in Fig. 11.

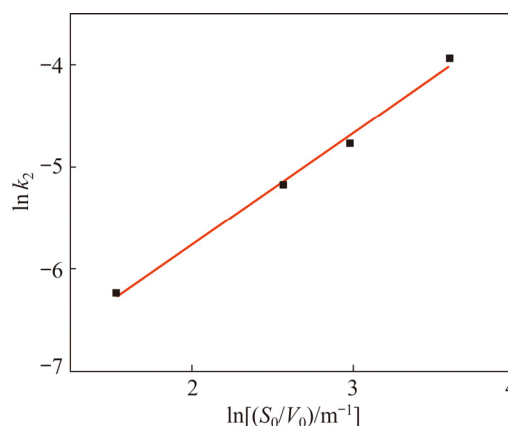


**Fig. 11** Diagram of  $\ln k_2$  vs  $\ln(S_0/V_0)$  under internal diffusion control at 525 °C

Figure 11 shows that the correlation coefficient of the fitting line is 0.9915, the frequency factor  $k'$  is 61.83, the shape factor  $n'$  is 0.55, and the correlation formula between  $k_2$  and  $(S_0/V_0)^2$  is

$$k_2 = 61.83 (S_0/V_0)^{1.1} \exp[-80175/(8.314T)] \quad (22)$$

Therefore, the kinetic equation of internal diffusion control is as follows:

$$1 - 2x/3 - (1-x)^{2/3} = 61.83 (S_0/V_0)^{1.1} \exp[-80175/(8.314T)] t \quad (23)$$

### 3.3.4 Critical conditions for control step changes

When the kinetic control step is changed from chemical reaction control to internal diffusion control, the internal diffusion rate and chemical reaction rate are the same, and the derivative of

oxidation ratio  $x$  with respect to time  $t$  of the two kinetic equations are respectively obtained as follows:

$$k_1 = \frac{1}{3}(1-x)^{-2/3} \frac{dx}{dt} \quad (24)$$

$$k_2 = -\frac{2}{3} \frac{dx}{dt} + \frac{2}{3}(1-x)^{-1/3} \frac{dx}{dt} \quad (25)$$

The oxidation ratio of the chemical reaction is  $x_0$  at this time, so,

$$x_0 = 1 - \left[ \left( \frac{1}{4} - \frac{k_2}{2k_1} \right)^{1/2} + \frac{1}{2} \right]^3 \quad (26)$$

Obviously,  $x_0$  increases with the increase of  $k_2/k_1$ . For molybdenite concentrate, the ratio of  $k_2/k_1$  is related to the particle size and reaction temperature. The smaller the particle size of molybdenite concentrate is, the larger the specific surface area is, and the larger the oxidation ratio controlled by chemical reaction will be at the same temperature. For any reaction, the chemical reaction rate is obviously faster than the internal diffusion reaction rate, so reducing molybdenite concentrate size can increase the proportion of chemical reaction and effectively improve the oxidation ratio of molybdenite. For the same particle size, with the increase of temperature, the oxidation ratio controlled by chemical reaction  $x_0$  decreases, but the overall reaction ratio significantly increases at high temperatures. Therefore, during the oxidizing roasting of molybdenite, the roasting temperature should be increased on the premise of minimizing volatilization.

### 3.3.5 Verification of kinetic model

To verify the developed kinetic model, a roasting experiment was conducted using the actual molybdenite concentrate. 5 g concentrate was roasted in a muffle furnace and its oxidation ratio curves were measured at 500 and 550 °C. At the same time, the particle size distribution of the concentrate was measured to calculate the specific surface area, and the oxidation ratio curves at 500 °C and 550 °C were calculated by the developed kinetic equation. The comparison of the measured and the calculated results is given in Fig. 12.

Figure 12 shows that the measured values by experiments are in good agreement with the calculated ones by the kinetic model in the early

and late stages of the reaction. In the middle stage, the measured values are higher than the calculated ones, which mainly is attributed to two reasons. First, when molybdenite is roasted in the muffle furnace, a large amount of concentrate is oxidized, leading to local overheating, so the reaction rate is accelerated. Secondly, when the control steps of the oxidation are changed, there is a transitional interval, where the reaction rate is between the two conditions and higher than the internal diffusion rate. Generally, the proposed kinetic model is basically consistent with the actual roasting process, which may provide a theoretical basis for the optimization design and numerical simulation of the oxidizing roasting process of molybdenite concentrate.

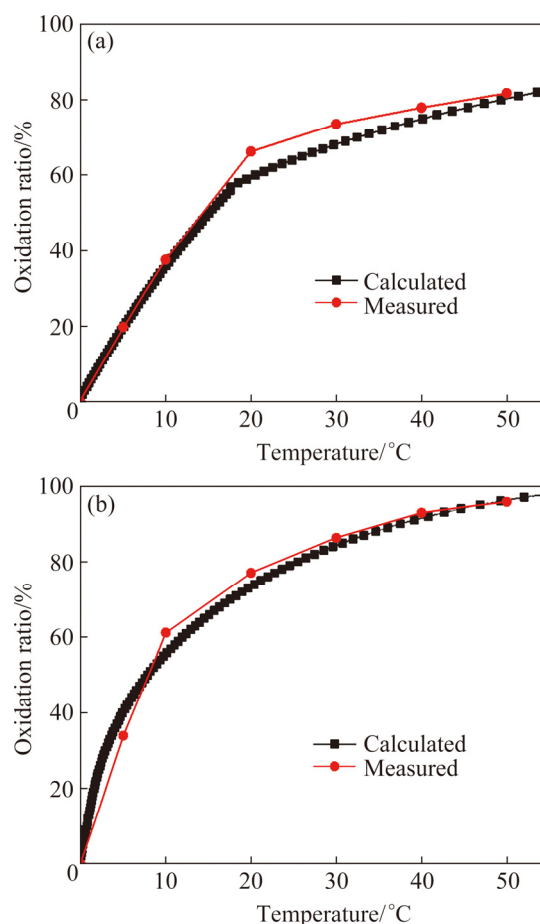


**Fig. 12** Comparison of measured and calculated oxidation ratios of molybdenite roasted at 500 °C (a) and 550 °C (b)

## 4 Conclusions

(1) Molybdenite begins to oxidize at 450 °C, and is oxidized rapidly above 500 °C under chemical reaction control with the apparent

activation energy of 123.18 kJ/mol, and the rate constant  $k_1$  of  $2.17 \times 10^5 (S_0/V_0 + 5.02) \exp[-123180/(8.314T)]$ . The oxidation rate correlates negatively to the molybdenite particle size.

(2) When the reaction rate reaches  $1 - [(1/4 - k_2/(2k_1))^{1/2} + 1/2]^3$ , the oxidation is controlled by the internal diffusion with the apparent activation energy of 80.175 kJ/mol and the constant  $k_2$  of  $61.83 (S_0/V_0)^{1.1} \exp[-80175/(8.314T)]$ . In this stage, reducing molybdenite particle size accelerates the internal diffusion of oxygen.

(3) Increasing roasting temperature is conducive to both the oxidation rate and desulfurization rate of molybdenite. The particle size determines the oxidation behavior of molybdenite concentrate. Reducing the particle size can effectively strengthen the oxidation roasting.

## Acknowledgments

The authors are grateful for the financial supports from the National Natural Science Foundation of China (52074364).

## References

- [1] HENNING W, WERNER O, KNUT B. Yellow pigment containing bismuth vanadate and taving the composition  $\text{BiVO}_{4-x}\text{Bi}_2\text{MoO}_{6-y}\text{Bi}_2\text{WO}_6$  [P]. US Patent 4455174. 1984.
- [2] NEMOTO Y, HASEGAWA A, SATOU M, ABE K, HIRAOKA Y. Microstructural development and radiation hardening of neutron irradiated Mo–Re alloys [J]. *Journal of Nuclear Materials*, 2004, 324(1): 87–93.
- [3] MEDVEDEV A S, ALEKSANDRO P V. Investigations on processing low-grade molybdenum concentrate by the nitric-acid method [J]. *Russian Journal of Non-Ferrous Metals*, 2009, 50(4): 353–356.
- [4] KHOLMOGOROV A G, KONONOVA O N. Processing mineral raw materials in Siberia: Ores of molybdenum, tungsten, lead and gold [J]. *Hydrometallurgy*, 2005, 76: 37–54.
- [5] WANG Si-fu, WEI Chang, DENG Zhi-gan, LI Cun-xiong, LI Xin-bing, WU Jun, WANG Ming-shang, ZHANG Fan. Extraction of molybdenum and nickel from Ni–Mo ore by pressure acid leaching [J]. *Transactions of Nonferrous Metals Society of China*, 2013, 23(10): 3083–3088.
- [6] MANOJ K, MANKHAND T R, MURTHY D S R, MUKHOPADHYAY R, PRASAD P M. Refining of a low-grade molybdenum concentrate [J]. *Hydrometallurgy*, 2007, 86: 56–62.
- [7] WARREN I H, MOUNSEY D M. Factors influencing the selective leaching of molybdenum with sodium hypochlorite from copper/molybdenum sulfide minerals [J]. *Hydrometallurgy*, 1983, 10: 343–357.
- [8] ANTONIJEVIC M M, PACOVIC N V. Investigation of molybdenite oxidation by sodium dichromate [J]. *Minerals Engineering*, 1992, 5(2): 223–233.
- [9] CAO Zhan-fang, ZHONG Hong, JIANG Tao, LIU Guang-yi, WANG Shuai. Selective electric-oxidation leaching and separation of Dexing molybdenite concentrates [J]. *The Chinese Journal of Nonferrous Metals*, 2013, 23(8): 2290–2295. (in Chinese)
- [10] ZHOU Qiu-sheng, YUN Wei-tao, XI Jun-tao, LI Xiao-bin, QI Tian-gui, LIU Gui-hua, PENG Zhi-hong. Molybdenite–limestone oxidizing roasting followed by calcine leaching with ammonium carbonate solution [J]. *Transactions of Nonferrous Metals Society of China*, 2017, 27(7): 1618–1626.
- [11] TRIPATHY P K, RAKHASIA R H. Chemical processing of a low grade molybdenite concentrate to recover molybdenum [J]. *Transactions of the Institutions of Mining and Metallurgy, Section C: Mineral Processing and Extractive Metallurgy*, 2006, 115(1): 8–14.
- [12] JUNEJA J M, SINGH S, BOSE D K. Investigation on the extraction of molybdenum and rhenium values from low grade molybdenite concentrate [J]. *Hydrometallurgy*, 1996, 41: 201–209.
- [13] KHOMOKSONOVA D P, BUDAIEVA A D, ANTROPOVA I G. Thermochemical decomposition of molybdenum concentrates with usage of magnesium-containing additives of natural origin [C]//IOP Conference Series: Earth and Environmental Science. Arnold Kirillovich Tulokhonov Ulan-Ude, 2019, 320, 012033.
- [14] ALEKSANDROW P, EDVEDVE A M, KADIROV A. Processing molybdenum concentrates using low-temperature oxidizing–chlorinating roasting [J]. *Russian Journal of Non-Ferrous Metals*, 2014, 55(2): 114–119. (in Russian)
- [15] ZLATANOVIC D, PURENOVIC M, ZEC S, MILJKOVIC M. The Role of NaCl in chlorine roasting of  $\text{MoS}_2$  [C]//Materials Science Forum. Trans Tech Publications, 1998: 282–349.
- [16] ALEKSANDROV P V, MEDVEDEV A S, MILOVANOV M F, IMIDEEV V A, KOTOVA S A, MOSKOVSKIKH D O. Molybdenum recovery from molybdenite concentrates by low-temperature roasting with sodium chloride [J]. *International Journal of Mineral Processing*. 2017, 161: 13–20.
- [17] MANKHAND T R, PRASAD P M. Lime-enhanced hydrogen reduction of molybdenite [J]. *Metallurgical Transactions B*, 1982, 13(2): 275–282.
- [18] PRASAD P M, MANKHAND T R, RAO P S. Lime-scavenged reduction of molybdenite [J]. *Minerals Engineering*, 1993, 6(8–10): 857–871.
- [19] AFSAHI M M, SOHRAHI M, EBRAHIM H A. A model for the intrinsic kinetic parameters of the direct reduction of  $\text{MoS}_2$  with hydrogen [J]. *International Journal of Materials Research*, 2008, 99: 1032–1038.
- [20] AFSAHI M M, SOHRAHI M, EBRAHIM H A. A study on the kinetics of hydrogen reduction of molybdenum disulfide powders [J]. *Thermochimica Acta*, 2008, 473: 61–67.
- [21] WANG Lu, ZHANG Guo-hua, DANG Jie, CHOU Kuo-chih. Oxidation roasting of molybdenite concentrate [J].

- Transactions of Nonferrous Metals Society of China, 2015, 25(12): 4167–4174.
- [22] GAN Min, FAN Xiao-hui, CHEN Xu-ling, WU Cheng-qian, JI Zhi-yun, WANG Song-rong, WANG Guo-jing, QIU Guan-zhou, JIANG Tao. Reaction mechanisms of low-grade molybdenum concentrate during calcification roasting process [J]. Transactions of Nonferrous Metals Society of China, 2016, 26(11): 3015–3023.
- [23] WILKMIRSKY I, OTERO A, BALLADARES E. Kinetics and reaction mechanisms of high-temperature flash oxidation of molybdenite [J]. Metallurgical and Materials Transactions B, 2010, 41(1): 3–73.
- [24] YANG Shuang-ping, GUO Shuan-quan, ZHANG Pan-hui, WANG Lei, ZHANG Xiao, HE Kai, LI Xue-wu, DANG Wen-jing. Kinetics of molybdenum in oxidation roasting process [J]. The Chinese Journal of Process Engineering, 2016, 16(6): 1016–102. (in Chinese)
- [25] BOSWELL P G. On the calculation of activation energies using a modified Kissinger method [J]. Journal of Thermal Analysis, 1980, 18(2): 353–358.
- [26] D'ARLAS B F, RUEDA L, STEFANI P M, de la CABA K, MONDRAGON I, ECEIZA A. Kinetic and thermodynamic studies of the formation of a polyurethane based on 1,6-hexamethylene diisocyanate and poly(carbonate-co-ester) diol [J]. Thermochimica Acta, 2007, 459(1–2): 94–103.
- [27] KANTARELIS E, YANU W, BLASIAK W, FORSQREN C, ZABANIOTOU A. Thermochemical treatment of E-waste from small household appliances using highly pre-heated nitrogen-thermogravimetric investigation and pyrolysis kinetics [J]. Applied Energy, 2011, 88(3): 922–929.
- [28] HU Rong-zu, SHI Qi-zhen. Thermal analysis kinetics [M]. Beijing: Science Press, 2001. (in Chinese)

## 不同颗粒尺寸辉钼矿的氧化焙烧动力学

李小斌, 吴涛, 周秋生, 齐天贵, 彭志宏, 刘桂华

中南大学 冶金与环境学院, 长沙 410083

**摘要:** 通过差热-热重实验和非等温分析法研究辉钼精矿的氧化焙烧动力学。结果表明: 高温焙烧有利于辉钼矿的氧化, 其初始氧化温度为 450 °C, 500 °C 以上时迅速氧化。氧化过程符合未反应收缩核模型。氧化初期受化学反应控制, 其表观活化能为 123.180 kJ/mol; 后期受内扩散控制, 表观活化能为 80.175 kJ/mol。整个氧化过程中辉钼矿的氧化速率和精矿的颗粒尺寸密切相关, 颗粒尺寸越小, 其氧化速率越大。

**关键词:** 辉钼矿; 氧化; 焙烧; 动力学; 颗粒尺寸

(Edited by Bing YANG)